A R C H I V E S O F M E T A L L U R G Y A N D M A T E R I A L S
Volume 60 2015 Issue 4
DOI: 10.1515/amm-2015-0482

R. MOLA*,#, S. MRÓZ**, P. SZOTA**, S. SAWICKI**

ANALYSIS OF THE DEFORMABILITY OF TWO-LAYER MATERIALS AZ31/EUTECTIC

ANALIZA MOŻLIWOŚCI ODKSZTAŁCANIA PLASTYCZNEGO MATERIAŁU DWUWARSTWOWEGO AZ31/EUTEKTYKA

The paper present the results of physical simulation of the deformation of the two-layered AZ31/eutectic material using the Gleeble 3800 metallurgical processes simulator. The eutectic layer was produced on the AZ31 substrate using thermochemical treatment. The specimens of AZ31 alloy were heat treated in contact with aluminium powder at 445°C in a vacuum furnace. Depending on the heating time, Al-enriched surface layers with a thickness of 400, 700 and 1100 μm were fabricated on a substrate which was characterized by an eutectic structure composed of the $Mg_{17}Al_{12}$ phase and a solid solution of aluminium in magnesium. In the study, physical simulation of the fabricated two-layered specimens with a varying thickness of the eutectic layer were deformed using the plane strain compression test at various values of strain rates. The testing results have revealed that it is possible to deform the two-layered AZ31/eutectic material at low strain rates and small deformation values.
Keywords: magnesium, alloyed layer, intermetallic phases, physical simulation, compession test

W pracy przedstawiono wyniki modelowania fizycznego odkształcania materiału dwuwarstwowego AZ31/eutektyka z wykorzystaniem symulatora procesów metalurgicznych Gleeble 3800. Warstwę o strukturze eutektyki wytworzono na podłożu ze stopu magnezu w gatunku AZ31 metodą obróbki cieplno-chemicznej. Próbki ze stopu AZ31 wygrzewano w kontakcie z proszkiem aluminium w temp. 445°C w piecu próżniowym. Zależnie od zastosowanego czasu wygrzewania uzyskano na podłożu magnezowym warstwy wzbogacone w aluminium o grubościach 400, 700, 1100 μm i strukturze eutektycznej składającej się z fazy międzymetalicznej $Mg_{17}Al_{12}$ oraz roztworu stałego aluminium w magnezie. W ramach symulacji fizycznych otrzymane dwuwarstwowe próbki o różnych grubościach warstwy eutektyki odkształcano stosując próbę ściskania w płaskim stanie odkształcenia przy różnych prędkościach odkształcenia. Otrzymane wyniki badań wskazują na możliwość odkształcania dwuwarstwowego materiału AZ31/eutektyka z małymi prędkościami odkształcenia oraz przy stosunkowo małych wartościach odkształcenia.

1. Introduction

Magnesium and its alloys exhibit a number of advantageous properties: high strength to weight ratio, high dimensional stability, high thermal conductivity, good workability and castability. However, insufficient corrosion and wear resistance have limited the practical application of these materials. Designing of new alloys or Mg-based composites is one of the possible routes to achieve better surface properties. The other way is applying surface treatment methods [1]. The promising method of surface treatment for improving of the corrosion and wear resistance of magnesium and its alloys is fabrication the Al-enriched surface layer on Mg substrate containing Mg-Al intermetallic phases. Al-enriched layer do not significantly increase the density of the substrate material. Finally, the recycling of coated elements with such layers is not complicated because aluminium is the main alloying element of Mg alloys. The techniques used to produce Al-enriched layers include: heating Mg-based components in contact with Al powder [2-5], electrodeposition [6], diffusion coating in molten salts [7,8], cold spray coupled with heat treatment [9], physical vapour deposition [10], laser processing [11,12]. Depending on the employed fabrication process and its parameters, the microstructure of the resulted coating may be composed of two continuous layers of intermetallic phases: the outer layer-Al_3Mg_2 and the inner layer-$Mg_{17}Al_{12,}$ or may have an eutectic structure of ($Mg_{17}Al_{12,}$ phase + solid solution of Al in Mg). There are also a lot of studies concerning the fabrication of Al-Mg bimetallic or Al-Mg-Al multi-layer products by hot-pressing [13, 14], extrusion [15-17], hot-rolling [18-20], cold-rolling [21] explosive cladding [22], twin-roll casting [23], in which the outer layer is either of pure aluminium or an aluminium alloy and can provide anti-corrosive protection. During fabrication of Al-Mg bimetallic

* KIELCE UNIVERSITY OF TECHNOLOGY, FACULTY OF MECHATRONIC AND MECHANICAL ENGINEERING, 7 TYSIĄCLECIA PAŃSTWA POLSKIEGO AV., 25-314 KIELCE, POLAND
** CZESTOCHOWA UNIVERSITY OF TECHNOLOGY, FACULTY OF PRODUCTION ENGINEERING AND MATERIALS TECHNOLOGY, INSTITUTE OF METAL FORMING AND SAFETY ENGINEERING, 19 ARMII KRAJOWEJ AV., 42-200 CZĘSTOCHOWA, POLAND
# Corresponding author: rmola@tu.kielce.pl

or Al-Mg-Al multilayer products, a transition diffusion zone of Mg-Al intermetallic phases may be formed at the bond interface. As shown in the literature, this intermetallic zone, being composed of the Al_3Mg_2 phase (on the Al side) and the $Mg_{17}Al_{12,}$ phase (on the Mg side), is hard and brittle, enhancing further the durability of such materials. For this reason, also the plastic forming of Mg-based elements with an Al-enriched surface layer composed of two continuous sub-layers of Mg-Al intermetallic phases is made very difficult.

The aim of this work was to study the possibility of plastic deformation of two-layered material AZ31/eutectic mixture. The Al-enriched layers with eutectic structure containing $Mg_{17}Al_{12,}$ phase were fabricated on AZ31 substrate by heating the specimens in contact with aluminium powder in vacuum furnace. The hot-working behaviour that material was determined in compression test performed in a temperature 420°C using Gleeble 3800 metallurgical processes simulator.

2. Experimental procedure

AZ31 alloy ingot was cut into rectangular specimens (50x20x12 mm). The macrostructure of the, i.e. the AZ31 alloy in an as-cast condition, is shown in Figure 1. The microstructure of the alloy consists of Mg-rich matrix and $Mg_{17}Al_{12,}$ phase located at grain boundary, furthermore, the dark precipitations can be observed in microstructure. According to EDS analysis, they contain Al and Mn (51.11 at. % Al, 29.16 at. % Mn, 19.73 at. % Mg) which indicates the Al-Mn-Mg phase.

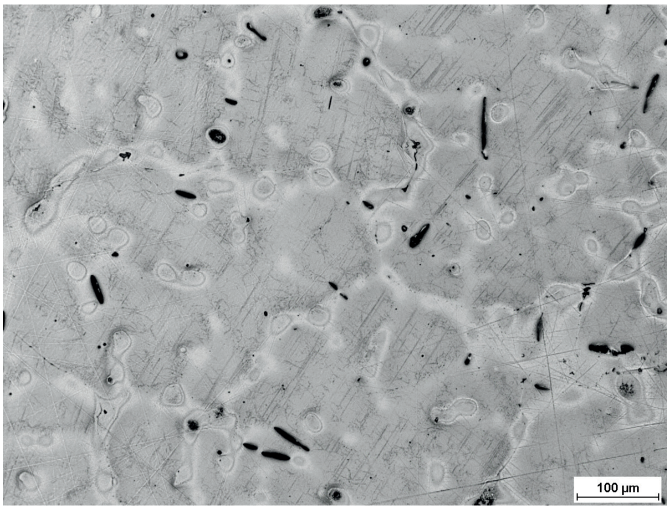

Fig. 1. Microstructure of AZ31 magnesium alloy cast billet

The process of fabrication eutectic layer on AZ31 substrate proceed as follows. The surface of the specimens were grinded using up to 800 grit SiC paper, cleaned with ethanol and then dried in air. The specimens were placed in steel container on a layer of dry aluminium powder and covered completely with more powder material. Then, the container was closed with the lid and placed in a vacuum furnace. The specimens were heated up from room temperature to 445°C for 30 min and hold at that temperature for 40, 60 and 90 min, and cooled down in the furnace to room temperature. The furnace was equipped with a pressure pad, which enabled the lid of the container to keep the powder pressed down tightly during heat treatment process.

The microstructure of the layers was observed using a Nikon ECLIPSE MA 200 optical microscope and a JEOL JSM-5400 scanning electron microscope. A chemical composition analysis was carried out by means of X-ray energy dispersive spectrometer (EDS) attached to SEM.

One of the methods enabling the determination of the plasticity of metals and alloys are physical simulations of processes, which are performed using different types of plastometers. Devices of this type enable the properties of deformed materials to be tested within a wide range of thermomechanical parameters, while allowing for the mode of increment of the specific strain-inducing force in time [24-26]. Developing the deformation schedules provides the capability to model the actual processes of plastic working of metals (such as rolling, pressing, forging, etc.) [24-26]. One of the types of devices with high testing capabilities is the Gleeble 3800 physical simulator. Therefore, the tests to determine the possibility of deforming the two-layered AZ31/eutectic mixture material were carried out using the above-mentioned device in the rectangular prism specimen compression test for a plane state of strain. It should be noted that the rectangular prism specimen compression test yields a three dimensional state of stress and a plane state of strain. This is a good approximation to the flat product rolling conditions. This assumption applies to homogeneous materials. By contrast, using the aforementioned method for two-layered specimens might cause a disturbance of the plane strain state. However, the compression method employed in the study was not used to determine the plastic flow curves for the material under examination, but only to establish the possibility of deforming two-layered materials, in which one of the layers contains hard intermetallic phases. The tests measured the magnitude of stress causing permanent deformations, which can be defined as the resistance to the plastic flow of the two-layered material. 10x15x20 mm specimens were used for the plastometric tests. The macrophotograph shown in Fig. 2 represents a view of the lateral surface of an example AZ31/eutectic mixture two-layered specimen prepared for compression tests using the Gleeble 3800 simulator. The eutectic layer produced on the AZ31 surface is characterized by a uniform thickness over the entire specimen length. The schedule of the compression test is shown in Fig. 3.

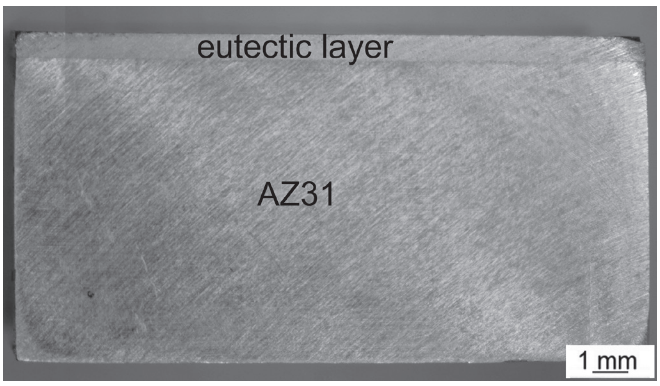

Fig. 2. The AZ31/eutectic specimen with an eutectic layer thickness of 1100 µm, fabricated by the thermochemical treatment method

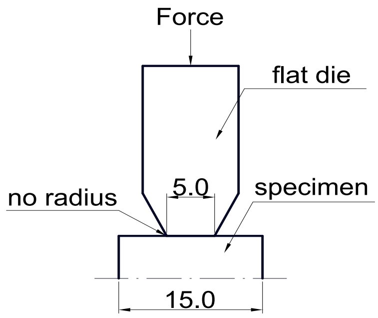

Fig. 3. The schedule of the rectangular prism specimen compression test using the Gleeble 3800 simulator

To reduce the effect of friction on the non-uniform specimen deformation, graphite pads and special graphite-based lubricant were put between the specimen faces and the tool surfaces. For the recording and control of temperature, two K-type thermocouples installed on the specimen lateral surface were used. The specimens were heated by a resistance method using anvils. To minimize the influence of scale on the determined parameters, the tests were performed in vacuum. The compression parameters, i.e. temperature, deformation and strain rate, were selected based on references [18-20, 27], where the Al-Mg-Al multi-layer material rolling process was investigated. The compression tests were conducted for the following parameters: temperature - 420ºC, strain rate - 0.1 s^{-1}; 1.0 s^{-1} and 10.0 s^{-1}, true deformation - from 0 to 0.1.

3. Results

3.1. Characterization of Al-enriched layers

The microstructure of the surface layer fabricated on the AZ31 substrate by heat treating the specimens in contact with aluminium powder at 445°C for 40 minutes is shown in Fig. 4. A uniform and continuous layer about 400 μm in thickness covers the AZ31 surface, as shown in Fig 4a. The layer had a typical eutectic structure (Fig. 4b) composed of a lighter and a darker phases. The eutectic structure of the layer suggests that the layer formation process proceeded trough a partial melting at the AZ31-substrate/Al-powder interface.

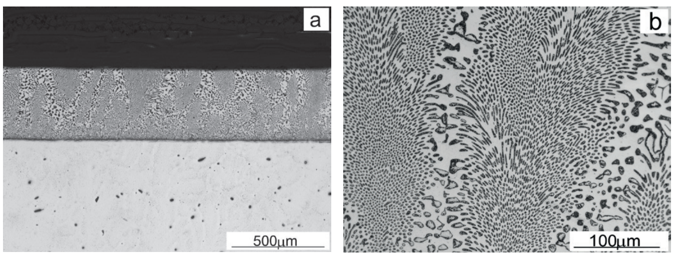

Fig. 4. An OM image of the layer formed on AZ31 substrate: (a) lower magnification, (b) details of the layer microstructure observed at higher magnification

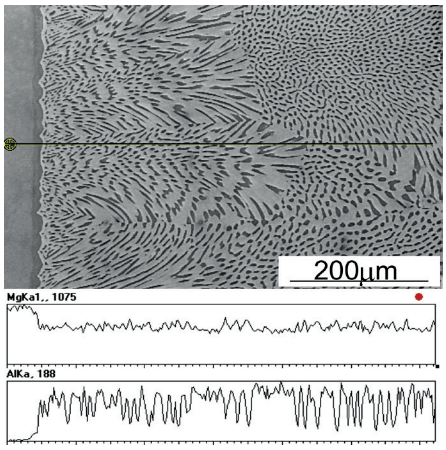

Fig. 5. SEM image showing the microstructure of the layer together with concentration of Mg and Al along the index line

The linear elemental distribution (Fig. 5) revealed that fabricated layer is enriched in aluminium. The result of the quantitative EDS analysis for lighter phase: 63.15 at. % Mg, 36.85 at. % Al, indicates an $Mg_{17}Al_{12}$ intermetallic phase development. The composition of darker phase: 86.62 at. % Mg, 13.48 at. % Al suggests a solid solution of aluminium in magnesium. As shown in Fig. 5 a thin transition zone can be observed between layer with eutectic structure and AZ31 substrate. The aluminium content in this area was about 8 at. % which indicates that Al-enriched layer is integrated with substrate by thin zone of a solid solution of aluminium in magnesium.

Fig. 6 presents the microstructure of the Al-enriched layers fabricated on AZ31 substrate after 60 min (Fig. 6a) and 80 min (Fig. 6b) of heat treatment. The longer the heating time, the thicker layer. A layer with a thickness about 700 and 1100 μm were produced at a temperature of 445°C for 60 and 80 min heating, respectively. As can be seen in these figures locally near the surface a white dendrites were observed in microstructure. The chemical composition of dendrites (62.64 at.% Mg, 37.36 at.% Al) is close to $Mg_{17}Al_{12,}$ intermetallic phase.

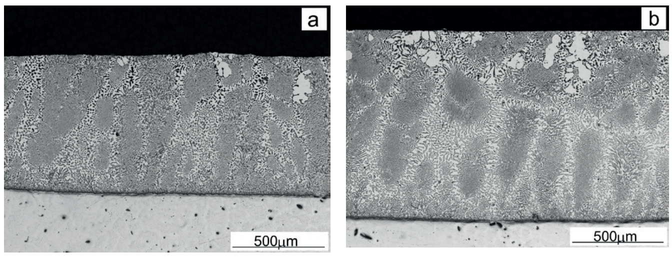

Fig. 6. OM images of the AZ31 specimens heat treated in contact with aluminium powder

The Al-enriched layer with eutectic structure had much higher hardness 185-205 HV0.1 as compared to 40 HV0.1 for AZ31 substrate.

3.2. Results of the physical simulation of the deformation of AZ31/eutectic two-layered material

The investigation into the possibility of deforming two-layered AZ31/eutectic specimens was divided into two stages. In the first stage, compression tests of two-layered specimens differing in eutectic layer thickness were performed at a constant deformation temperature. The dimensions of the specimens used were identical. The temperature, at which the compression test was performed, was 420°C. The first specimen had an eutectic layer thickness of 400 μm; the second one, 700 μm; while the last one, 1100 μm. For each of the deformed specimens, a constant deformation value of 0.1, and a constant strain rate value of 1 s^{-1}, were assumed. To compare the results obtained for the two-layered specimens, a compression test was additionally performed on a single-layered specimen made of the AZ31 magnesium alloy and having dimensions corresponding to those of the two-layered specimens. The purpose of the test was to refer the results obtained for the two-layered specimens to the single-layered AZ32 alloy specimen.

Figure 7 illustrates the results of the tests of compression of three two-layered AZ31/eutectic specimens with a varying eutectic layer thickness and a specimen of the AZ31 magnesium alloy. The data shown in Fig. 7 indicate that the resistance to specimen plastic flow, as defined by the stress magnitude, is identical to all of the two-layered specimens, regardless of the eutectic layer thickness. The slight differences in the plastic flow curves occur in the deformation range from 0.005 to 0.03, which is due to the eutectic layer thickness effect. During compression testing in a deformation range of up to 0.03, the eutectic layer is plastic enough to create a deformation resistance, while with increasing deformation magnitude, this layer cracks at the location of sharp anvil edges. The cracking of the eutectic surface results in a reduction of the flow stress and plastic resistance of the deformed two-layered specimen.

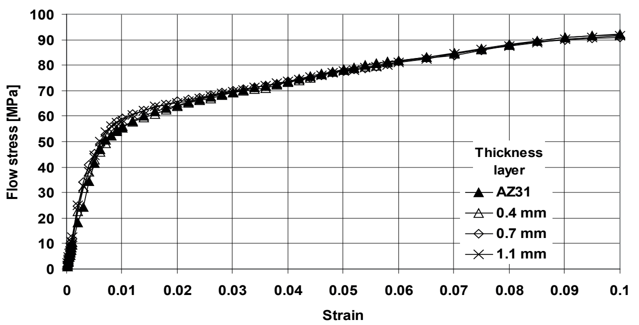

Fig. 7. The plastic flow curves obtained from the compression testing of two-layered AZ31/eutectic specimens and an AZ31 magnesium alloy specimen at a temperature of 420°C and a strain rate of 1 s^{-1}

The presented plastic flow curve for the AZ31 magnesium alloy specimen in the deformation range from 0.03 to 0.1 coincides with the curves for the two-layered specimens. This is indicative of the fact that during the two-layered specimen compression test it is the AZ31 magnesium alloy layer that largely deforms, as confirmed by the coinciding plasticity curves for the specimens tested. The hardness measurements of the eutectic and AZ31 alloy layer have shown that the eutectic layer has a hardness value that is 5 times that of the AZ31 alloy. The eutectic hardness is approx. 190 HV0.1, while the hardness of the AZ31alloy is only approx. 40 HV0.1. The microscopic measurements of variations in eutectic layer thickness confirmed the absence of deformation of this layer – the eutectic layer thickness on the anvil-affected surface did not change.

Figure 8 shows the cross-sections of deformed two-layered specimens with the eutectic layer of varying thickness. The shape of the employed anvil (no rounding at the location of the working portion passing into the lateral surface – Fig. 3) causes significant tensile stresses to occur at the anvil–eutectic interface as the anvil penetrates into the tested material, which results in a break of the eutectic layer. Cracks in the eutectic layers propagating perpendicularly to the substrate were observed in the regions of anvil penetration into the eutectic layers, as well as on the specimen side edges, which did not come into contact with the anvil working surface. This result suggest that for the assumed deformation–temperature parameters, regardless of the eutectic layer thickness, this layer is not plasticized.

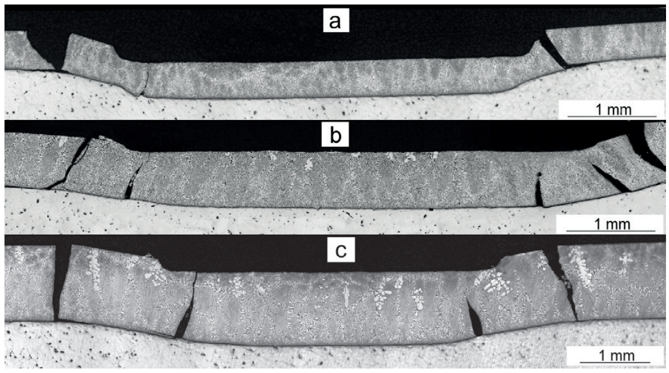

Fig. 8. Two-layered AZ31/eutectic specimens with varying eutectic layer thickness after the compression test at a temperature of 420°C (strain rate, 1 s^{-1}; deformation, 0.1): a) 400 μm, b) 700 μm, c) 1100 μm

In the second testing stage, two-layered material compression tests were performed at a temperature of 420°C for specimens with an eutectic layer thickness of 700 μm, using different strain rates, namely: 0.1, 1.0 i 10 s^{-1}. The compression tests were carried out on the assumption that the deformation would be 0.1. Comparison of the obtained plastic flow curves is shown in Fig. 9.

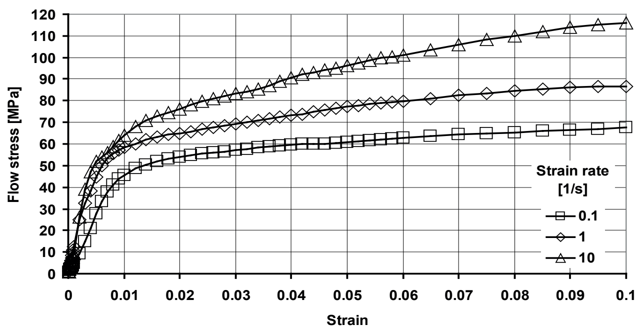

Fig. 9. The plastic flow curves obtained from the compression tests of two-layered AZ31/eutectic specimens with an eutectic layer thickness of 700 μm for different strain rates

From the data represented in Fig. 9 it can be noticed that the strain rate has a considerable influence on the values of stress recorded during the deformation of the material tested. By examining the effect of strain rate on the magnitude of plastic flow resistance it has been found that with the increase in strain rate the resistance to the plastic flow of deformed two-layered specimens increases. The analysis of the data in Figs. 7 & 9 shows that the recorded stress values are dependent on the strain rate. The high hardness and brittleness of the eutectic layer causes this layer, as a result of the preset deformation, to undergo fragmentation, similarly as in the two-layered specimens shown in Fig. 8. In spite of the absence of eutectic layer influence on the stress value, performed metallographic examination showed a significant effect of strain rate on the eutectic layer fragmentation. The microstructures of the two-layered specimens after the compression test at varying strain rates are shown in Fig. 10.

The data represented in Fig. 10a show that using the highest strain rate (10 s^{-1}) has resulted in a considerable fragmentation of the eutectic layer. During the compression test, similarly as for the specimens shown in Fig. 8., a break in the eutectic layer has occurred in the sharp anvil edge-affected locations. Cracks propagating perpendicularly to the substrate occurred over the entire eutectic layer length affected by the flat anvil surface. In order to minimize the likelihood of cracks occurring in the eutectic layer, the strain rate was reduced to a level of 1 and 0.1 s^{-1} (Figs. 10b and 10c), respectively. Figure 10b shows a macrophotograph of a specimen deformed at a temperature of 420°C at a strain rate of 1 s^{-1}. In this case it was observed that cracks in the eutectic layers occurred locally, only in the locations of anvil penetration into the specimen being deformed. No cracks were noted in the central part of the compressed specimen zone. Moreover, the frequency of their occurrence decreased considerably compared to the specimen shown in Fig. 10a. A macrophotograph of the specimen deformed at a strain rate of 0.1 s^{-1} is shown in Fig. 10c. On the cross-section, only two cracks are visible near the locations of anvil penetration into the two-layered specimen. After taking measurements of the thickness of the eutectic layer after the compression test, its thinning in the compressed zone (Fig. 10c) was observed. The thickness of the eutectic layer prior to the deformation was 700-710 μm, while after the deformation, 630-650 μm. For specimens deformed at higher strain rate, no change in the thickness of the eutectic layer was noted (Figs. 10a & 10b), which indicates the absence of deformation of this layer. The obtained results show that at the temperature 420°C and with the use of small strain rates it is possible to deform the two-layered AZ31/eutectic material.

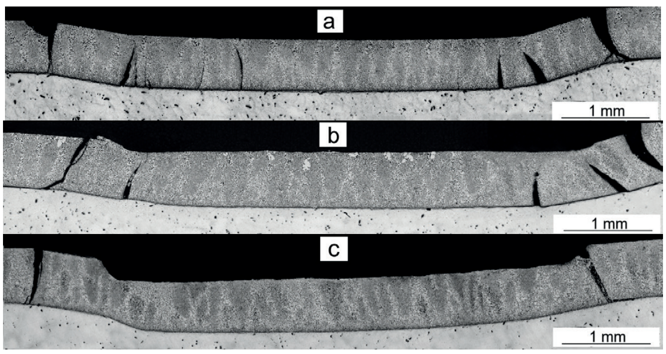

Fig. 10. Two-layered AZ31/eutectic specimens with an eutectic layer thickness of 700 μm after the compression test at a temperature of 420°C, deformation of 0.1 and a strain rate of, respectively: a) 10 s^{-1}, b) 1 s^{-1}, c) 0.1 s^{-1}

The analysis of the data in Figs. 8 and 10 shows that in none of the examined cases was a separation of the eutectic layer from the magnesium substrate observed, which suggests its strong metallurgical bonding with the substrate. Cracks in the eutectic layer always propagated in parallel to the direction of the preset deformation.

4. Conclusions

The layers with a structure of an eutectic mixture (($Mg_{17}Al_{12}$ + solid solution of aluminium in magnesium) were fabricated on the AZ31 alloy surface by heating the substrate in contact with aluminium powder. The produced eutectic layers were distinguished by high hardness compared to the AZ31 magnesium alloy substrate. The performed compression tests have shown that the resistance to the plastic flow of two-layered specimens composed of AZ3 alloy and a top eutectic layer is dependent solely on the properties of the softer component, in this case the AZ31 magnesium alloy. Due to its low plasticity and high hardness, the eutectic layer undergoes fragmentation during deformation, while not losing the integration of bonding with the AZ31 alloy. The obtained investigation results indicate the possibility of deforming the two-layered AZ31/eutectic material at low strain rates and with relatively small deformation values.

REFERENCES

[1] J.E. Gray, B. Luan, J. Alloys and Compd. **336**, 88 (2002).
[2] I. Shigematsu, M. Nakamura, N. Saitou, K. Shimojima, J. Mater. Sci. **19**, 473 (2000).
[3] L. Zhu, G. Song, Surf Coat Technol. **200**, 2834 (2006).
[4] R. Mola, Archives of Metallurgy and Materials **59**, 4, 1409 (2014).
[5] R. Mola, K. Jagielska-Wiaderek, Surf. Interface Anal. **46**, 121 (2014).
[6] H. Yang, X. Guo, G. Wu, W. Ding, N. Birbilis, Corros. Sci. **53**, 381 (2011).
[7] C. Zhong, M. He, L. Liu, Y. Wu, Y. Chen, Y. Deng, B. Shen, W. Hu, J. Alloys Compd. **504**, 377 (2010).
[8] M. He, L. Liu, Y. Wu, Z. Tang, W. Hu, J. Coat. Technol. Res. **6**(3) 407 (2009).
[9] K. Spencer, M. X. Zhang, Scripta Mater. **61**, 44 (2009)
[10] M.A. Taha, N.A. El-Mahallawy, R.M. Hammouda, S. I. Nassef, J. Coat. Technol. Res. **7**(6) 793 (2010).
[11] A. Singh, S.P. Harimkar, JOM **64**(6), 716 (2012).
[12] S. Ignat, P. Sallamand, D. Grevey, M. Lambertin, Appl. Surf. Sci. **225**, 124 (2004).
[13] X. Li , W. Liang, X. Zhao, Y. Zhang, X. Fu, F. Liu, J. Alloys Compd. **471**, 408 (2009).
[14] B. Zhu, W. Liang, X. Li, Mater. Sci. Eng. A **528**, 6584 (2011).
[15] T. Tokunaga, K. Matsuura, M. Ohno, Mat. Trans. **53**, 1034 (2012).
[16] T. Tokunaga, M. Pietrzyk, K. Matsuura, O. Munekazu, 11th World Congress on Computational Mechanics (WCCM XI), Barcelona (2014).
[17] S. Boczkal, P. Korczak, B. Plonka, W. Szymański,

M. Nowak, Magnesium Technology 2014, Ed. by: M. Alderman, M.V. Manuel, N. Hort, and N.R. Neelameggham, San Diego, 285 (2014).

[18] H. Chang, M.Y. Zheng, W.M. Gan, K. Wu, E. Maawad, H.G. Brokmeier, Scripta Mater. 61, 717 (2009).

[19] X. P. Zhang, T.H. Yang, S. Castagne, J.T. Wang, Mater. Sci. Eng. A **528**, 1954 (2011).

[20] Ch. Luo, W. Liang, Z. Chen, J. Zhang, Ch. Chi, F. Yang, Mater. Chatact. **84**, 34 (2013).

[21] H. Matsumoto, S. Watanabe, S. Hanada, J. Mater. Process. Technol. **169**, 9 (2005).

[22] S. Mroz, G. Stradomski, H. Dyja, A. Galka, Arch. Civil Mech. Eng. **15**(2), 317 (2015).

[23] J.H. Bae, A.K. Prasada Rao, K.H. Kim, N.J. Kim, Scripta Mater. **64**, 836 (2011).

[24] H. Dyja, A. Galkin, M. Knapinski, Reologia metali odkształconych plastycznie, Czestochowa, 2014 (in Polish).

[25] F. Grosman, E. Hadasik, Technologiczna plastyczność metali, Gliwice 2005 (in Polish).

[26] E. Hadasik, Badania plastyczności metali, Gliwice 2008 (in Polish).

[27] W.P. Li, H. Zhou, Z.F. Li, J. Alloys Compd. **475**, 227 (2009).

Received: 20 November 2014.